Superconductivity on the threshold of magnetism in $CePd_2Si_2$ and $CeIn_3$

F M Grosche[1], I R Walker, S R Julian, N D Mathur, D M Freye, M J Steiner and G G Lonzarich

Cavendish Laboratory, Madingley Road, Cambridge CB3 0HE, UK

Abstract
The magnetic ordering temperature of some rare-earth-based heavy-fermion compounds is strongly pressure dependent and can be completely suppressed at a critical pressure, p_c, making way for novel correlated electron states close to this quantum critical point. We have studied the clean heavy-fermion antiferromagnets $CePd_2Si_2$ and $CeIn_3$ in a series of resistivity measurements at high pressures up to 3.2 GPa and down to temperatures in the mK region. In both materials, superconductivity appears in a small window of a few tenths of a GPa on either side of p_c. We present detailed measurements of the super-conducting and magnetic temperature–pressure phase diagram, which indicate that superconductivity in these materials is enhanced, rather than suppressed, by the closeness to magnetic order.

1. Introduction

The intense Coulomb interaction and low bandwidth driving electronic correlations in heavy-fermion systems lead to a fascinating variety of low-temperature states that remain only partly understood. In analogy with liquid ^{3}He, but at a new level of complexity and diversity, the effective quasiparticle interaction responsible for the high scattering rates and effective masses of these systems could for suitable quasiparticle spin orientation become attractive enough to foster unconventional superconductivity.

Increased and widespread interest in these compounds arose when superconductivity was indeed discovered in the heavy-fermion compound $CeCu_2Si_2$ [1], which is now known to rest on the border of magnetic order at ambient pressure, and can be moved into the magnetic state by suitable sample preparation or doping [2–4]. Further convincing evidence for the closeness of this material to magnetic order emerges from high-pressure measurements on the isoelectronic and isostructural relative $CeCu_2Ge_2$ [5]. Magnetism makes way in this material to superconductivity at a pressure just sufficient to reduce the unit-cell volume to that of $CeCu_2Si_2$ at ambient pressure.

The close association of superconductivity with the vanishing of a magnetic phase in $CeCu_2Si_2/Ge_2$ prompts the question of whether the two types of order are simply in competition,

---

as would be suggested for a conventional pairing scenario, or whether they could be related, as is suggested by the analogy with liquid ^{3}He. In the former case, the proximity of the two phases would be purely accidental, whereas in the latter an attractive magnetic component of the quasiparticle interaction could contribute to forming a superconducting state close to the threshold of magnetism. In this *magnetic interaction* scenario, spin fluctuations effectively replace lattice vibrations in binding the heavy quasiparticles into Cooper pairs. As this interaction is dominant only close to the border of magnetism, one might expect to find superconductivity typically only over a narrow region in lattice density, connected to the disappearance of magnetic order and extending to both sides of the critical point, at least when the transition is continuous. By contrast, the superconducting region in $CeCu_2Si_2/Ge_2$ extends over nearly 10 GPa in pressure to the high-pressure side of the critical point, suggesting a more complicated origin for superconductivity in this case.

This observation and the extensively studied metallurgical peculiarities of the $CeCu_2Si_2$ system motivate a search for related but simpler materials. Strikingly, nearly two decades of research into Ce-based heavy-fermion compounds failed to bring up any other super-conductors, raising the question of why superconductivity should be so narrowly confined to the $CeCu_2Si_2/Ge_2$ system.

Within the magnetic interaction picture, one may expect to find such candidates by tuning magnetically ordered compounds through the point where the ordering temperature falls continuously to zero. The study of these *quantum critical points* has a history dating back to theoretical and experimental work on d metals [6–16]. Recently, the systematic investigation of the magnetic quantum critical point in Ce-based systems has brought to light a host of pure compounds which show a tendency towards superconductivity when they are tuned through the threshold of magnetism as a function of lattice density by means of hydrostatic pressure ($CePd_2Si_2$ [17], $CeRh_2Si_2$ [18], $CeCu_2$ [19], $CeIn_3$ [20] and possibly also $CeCu_5Au$ [21]).

In this paper, we concentrate on two of these materials, the tetragonal $CePd_2Si_2$, which was the first Ce-based heavy-fermion superconductor to be found outside the $CeCu_2Ge_2/Si_2$ system, and the cubic $CeIn_3$. In both materials we find a narrow superconducting region of only a few tenths of a GPa around the critical pressure, p_c, where the antiferromagnetic ordering temperature extrapolates to zero. Detailed investigations of their normal and superconducting properties, in particular by means of neutron scattering, are complicated by the need to use hydrostatic pressure to suppress magnetic order. Fortunately, $CeNi_2Ge_2$, the isoelectronic relative of $CePd_2Si_2$, has been found to display at ambient pressure a behaviour analogous to that of $CePd_2Si_2$ just beyond the critical pressure [23–25]. Studies on $CeNi_2Ge_2$ enable us to extend the phase diagram of $CePd_2Si_2$ to higher effective pressure and to examine the evolution of the normal state and novel ordered states in greater detail [24–29]. The resulting phase diagram shows not only a low-pressure superconducting phase, limited to a small pressure range similar to that observed for $CePd_2Si_2$, but also an unexplored magnetic phase arising at high pressures of the order of 1.5 GPa and coinciding with a further superconducting region at high pressure, which extends up to at least about 3 GPa. This leads us to expect a similar second superconducting region in the sister compound $CePd_2Si_2$ starting at pressures about 1.5 GPa above p_c, i.e. above 4 GPa and stretching to about 3 GPa above p_c, up to around 6 GPa. Unfavourable sample or pressure conditions may in some cases cause the two superconducting ranges to merge, giving rise to the impression of a single, wide superconducting phase.

The merging of two superconducting ranges under non-hydrostatic pressure would offer an explanation for the drastic contrast between Bridgman-cell measurements on $CePd_2Si_2$ using a solid pressure medium [30], which show a wide superconducting region above p_c, and both our original determination of the phase diagram in a hydrostatic pressure cell [31] and its recent independent confirmation [32, 33]. While unsuitable for detailed studies of the

critical region, where under *hydrostatic* conditions, a very narrow superconducting region can clearly be resolved, the Bridgman-cell measurements give a first indication of the possible presence of a second high-pressure superconducting phase in CePd$_2$Si$_2$, as anticipated from earlier findings on CeNi$_2$Ge$_2$ [24–29].

These findings on CeNi$_2$Ge$_2$ and CePd$_2$Si$_2$ raise the intriguing possibility that some tetragonal cerium heavy-fermion compounds could be nearly critical over a wide region in parameter space, pressure or composition, maybe as a result of the competition between different types of magnetic order. This scenario may present the simplest and most intuitive explanation for the surprising stability of superconductivity in CeCu$_2$Si$_2$.

1.1. CePd$_2$Si$_2$ and CeIn$_3$

The heavy-fermion antiferromagnets CePd$_2$Si$_2$ and CeIn$_3$ offer an interesting opportunity for studies of the antiferromagnetic heavy-fermion critical point. CePd$_2$Si$_2$ is isostructural to the heavy-fermion superconductor CeCu$_2$Si$_2$ [1] and its larger-volume relative CeCu$_2$Ge$_2$ [5] (ThCr$_2$Si$_2$ structure), but differs from CeCu$_2$Si$_2$ in the number of d electrons in the d-metal constituent, and hence in the character of the Fermi surface and in the magnetic properties. At ambient pressure, CePd$_2$Si$_2$ orders in an antiferromagnetic structure below a Néel temperature T_N of about 10 K with a comparatively small moment of $\simeq 0.7\,\mu_B$ [34]. The spin configuration consists of ferromagnetic (110) planes with spins normal to the planes and alternating in directions along the spin axis. Previous high-pressure measurements indicate that T_N is strongly pressure dependent in CePd$_2$Si$_2$ and has a critical pressure within the range of conventional hydrostatic pressure cells [35].

The discovery of superconductivity in CeIn$_3$ provides a cubic reference material which may be simpler to describe theoretically. CeIn$_3$ crystallizes in the cubic AuCu$_3$ structure and orders at ambient pressure near 10 K with the ordering wavevector in the (111) direction [22].

Here, we describe the results of a detailed study of the critical region, where the antiferromagnetic ordering temperature T_N falls to zero as a function of pressure, in both CePd$_2$Si$_2$ and CeIn$_3$ (figures 1 and 2). Both materials display a very narrow superconducting region close to p_c, but the shapes of the superconducting phase lines, $T_c(p)$, differ slightly. Moreover, close to the critical pressure, the normal-state resistivity, ρ, in CeIn$_3$ approaches the low-temperature limiting form $\Delta\rho \equiv \rho - \rho_0 \propto T^{3/2}$, where ρ_0 denotes the residual resistivity, smoothly. By contrast, in CePd$_2$Si$_2$ the resistivity is nearly linear over almost two orders of magnitude in temperature. Moving away from p_c, a Fermi-liquid T^2-resistivity appears to return more rapidly in CeIn$_3$ than in CePd$_2$Si$_2$.

2. Experimental techniques

We have used pressure as the exclusive control parameter in a study of the stoichiometric heavy-fermion compounds CePd$_2$Si$_2$ and CeIn$_3$ to minimize possible complications due to impurities or disorder. As the critical pressure in these compounds lies within the range of conventional piston–cylinder clamp cells, full advantage can be taken of the high-pressure homogeneity and hydrostaticity available with this method, which makes possible a detailed study of the phase lines $T_c(p)$ over a very narrow pressure range. The electrical resistivity at pressures up to about 3.2 GPa was measured by a low-power AC four-terminal method inside BeCu/maraging steel hydrostatic clamp cells filled with a 1:1 mixture of iso-pentane and n-pentane. The pressure was obtained to within ±0.1 kbar from the resistively determined superconducting transition temperature of a tin sample [36]. The sample resistance was scaled to published values for the
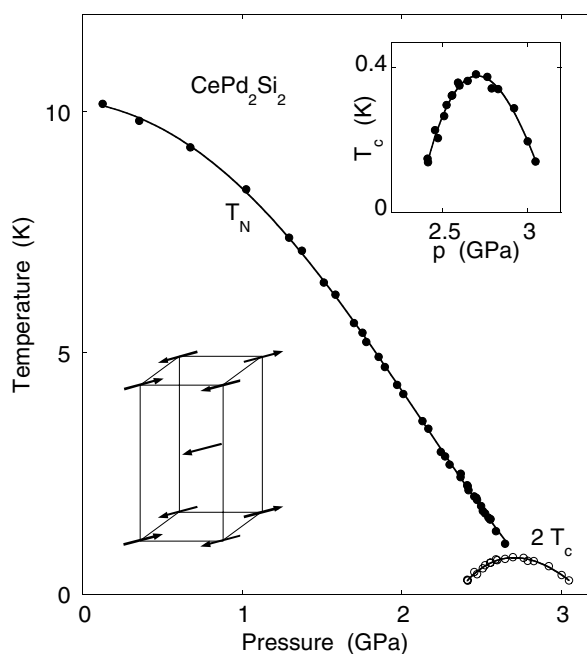
Figure 1. The pressure–temperature phase diagram of CePd$_2$Si$_2$. Magnetic (T_N) and super-conducting (T_c) transition temperatures have been determined from the mid-points of dρ/dT and ρ, respectively. The inset shows the superconducting part of the phase diagram in more detail. As can be inferred from figure 4, later, the transition width, ΔT_c, is typically of the order of 50 mK, but rises towards the high- and low-pressure borders of the superconducting region.

room temperature resistivity to obtain an absolute resistivity scale[2]. Experiments were carried out using a top-loading dilution refrigerator and an adiabatic demagnetization refrigerator. Single crystals of CePd$_2$Si$_2$ and CeIn$_3$ were prepared by a radio-frequency melting technique in a water-cooled copper crucible and UHV chamber in which ultrapure argon under pressures of up to 8 bar was introduced for part of the process. Further details of the preparation process and of the sample characterization are given in [37]. The residual resistivity ratio $\rho(300 \text{ K})/\rho(T \rightarrow 0 \text{ K})$ is approximately 50 at atmospheric pressure for the best crystals of CePd$_2$Si$_2$ and 100 for CeIn$_3$. Apart from the comparative study on the role of sample quality shown in figure 5(b) later, all of the results on CePd$_2$Si$_2$ were obtained on a single specimen with a resistance ratio RRR $\equiv \rho(300 \text{ K})/\rho_0 \simeq 34$ ($\rho_0 \simeq 1.4 \ \mu\Omega$ cm). A common problem in the preparation of CeIn$_3$ is the inclusion of small amounts of indium in the sample. Care was taken to achieve vigorous stirring during the initial stages of preparation. Samples were then checked for the presence of In inclusions by resistivity measurements below 4 K. The superconducting phase diagram presented here was recorded on a sample with a minimal amount of second phase, which is detected as an anomaly of order 1% in the resistivity trace. A second sample with similar residual resistivity (0.6 $\mu\Omega$ cm versus 0.7 $\mu\Omega$ cm), but no detectable indium inclusion was used in studying the normal-state properties, and in confirming the phase diagram at selected pressures.

---

[2] For CePd$_2$Si$_2$, the a-axis resistivity at ambient pressure was scaled to the room temperature value given in [30], $\rho(300 \text{ K}) = 47 \ \mu\Omega$ cm, while for CeIn$_3$, we assumed $\rho(300 \text{ K}) = 20 \ \mu\Omega$ cm for the ambient-pressure resistivity, following [22].
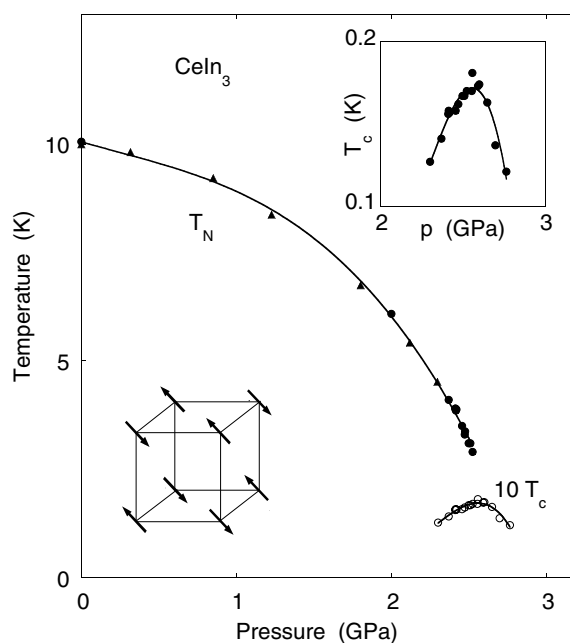
Figure 2. The pressure–temperature phase diagram of CeIn$_3$. Magnetic (T_N) and superconducting (T_c) transition temperatures have been determined from the mid-points of dρ/dT and ρ, respectively. The solid triangles have been taken from [22], scaling the pressure axis by a fixed factor of about 90%. The different absolute pressure scale evident from [22] is attributed to differences in the pressure calibration. The inset shows the superconducting part of the phase diagram in more detail. The transition width, ΔT_c, is only weakly pressure dependent and remains smaller than 20 mK where it could be determined.

3. Results

Resistivity measurements, while difficult to interpret quantitatively, can give important qualitative information. In heavy-fermion systems, the high-temperature resistivity is usually large ($\sim$50 $\mu\Omega$ cm) and only weakly temperature dependent, consistent with the scattering of charge carriers off thermally disordered moments. As the temperature is lowered, this scattering begins to drop significantly at an upper temperature scale, T_{sf}, below which thermal fluctuations of the local magnetic order parameter are increasingly frozen out. At low enough temperature, below a scale T_{FL}, most materials approach the low-temperature limiting forms predicted by Fermi-liquid theory, which should give an electronic contribution to the resistivity $\Delta\rho \propto T^2$. However, the spin degrees of freedom may also condense into magnetically ordered states at ordering temperatures T_m (T_N in the antiferromagnetic case), leading to further decreases in magnetic scattering, and consequently to anomalies or kinks in the resistivity trace at low temperatures. In addition, the formation of an antiferromagnetically ordered state can be accompanied by the opening of a charge gap over a section of the Fermi surface, which may be visible as an increase in the resistivity on cooling, when measured along particular crystal orientations. Important information on the nature of the normal state can be gained by examining the low-temperature form of $\rho(T)$. In a number of materials on the border to magnetism one finds $\Delta\rho \propto T^x$ with $x < 2$. This is evidence for an anomalous quasiparticle scattering mechanism, which appears to go beyond the regular quasiparticle interaction on which conventional Fermi-liquid theory is based.

3.1. CePd$_2$Si$_2$

The resistivity of CePd$_2$Si$_2$ exhibits a very strong pressure dependence (figure 3). We can identify three main features. Firstly, a sharp kink occurs in the resistivity at a temperature T_N, which coincides, at zero pressure, with the antiferromagnetic ordering temperature (or Néel temperature) deduced from neutron experiments, $T_N(p = 0) \simeq 10.2$ K [34]. The position of the kink in the resistivity is assumed to correspond to the Néel temperature also at higher pressures. T_N decreases with increasing pressure and falls below 1 K at around 2.6 GPa. Above about 1.5 GPa, this decrease is nearly linear with a slope of -4.8 K GPa^{-1}, and extrapolates to a critical pressure p_c of 2.86 GPa (figure 1). This linear pressure dependence $T_N \propto (p_c - p)$ is not consistent with conventional spin-fluctuation predictions for a three-dimensional antiferromagnet, where one would naively expect $T_N \propto (p_c - p)^{z/d} = (p_c - p)^{2/3}$ [6]. Here, z denotes the dynamical exponent, usually assumed to be 2 in the antiferromagnetic case, and d is the dimensionality of the spin-fluctuation spectrum. A linear pressure dependence of T_N would in this model rather point towards $d = 2$, or at least indicate a very anisotropic spin-fluctuation spectrum.
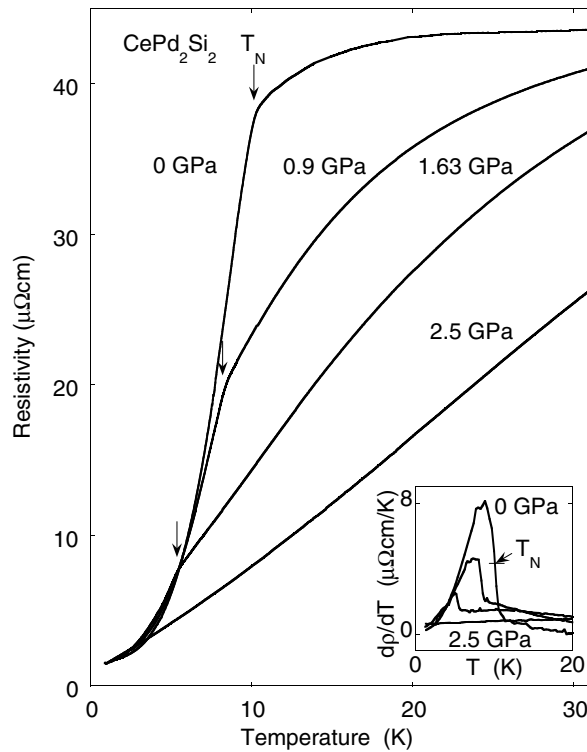

Figure 3. The temperature dependence of the resistivity, ρ, of CePd$_2$Si$_2$ measured along the *a*-axis at different pressures. The Néel temperature, T_N, marked by arrows, is extracted as the mid-point of the sudden change in the slope of $\rho(T)$, dρ/dT (inset).

Secondly, the behaviour of the resistivity above T_N changes dramatically with pressure. At zero pressure, the resistivity stays constant to within 10% from room temperature down to the Néel temperature, below which it falls sharply to a small residual value. At higher pressures, the resistivity develops a progressively stronger temperature dependence in the normal state. In particular, the temperature of the 'shoulder', below which the resistivity falls off, increases

rapidly with pressure. The resistivity curves for $T > T_N$ appear to scale roughly with a characteristic temperature which we associate with the spin-fluctuation temperature T_{sf}.

Thirdly, we can identify a small linear region in the resistivity just above T_N even at zero pressure. At higher pressures, this region expands until, near the critical pressure, we observe a quasi-linear resistivity over a wide range in temperature. More precisely, the low-temperature form of the resistivity of $CePd_2Si_2$ follows a power law $\rho = \rho_0 + AT^x$, where x is a heuristic exponent close to 1 (figure 8—see later). This power-law dependence of the resistivity characterizes the sample response over nearly two orders of magnitude in temperature up to about 40 K, where $\rho(T)$ crosses over to a nearly constant high-temperature value above 100 K (figure 8, later). Comparing samples of different ρ_0 has revealed a variation of the exponents in the range $1.1 < x < 1.5$ and a general trend towards lower values for purer specimens, indicating a possible limiting value of 1 for ideally pure samples [24, 25]. This behaviour persists up to about 3.2 GPa, which is the pressure range accessible in this study, and no return to a Fermi-liquid form of the resistivity could be observed at low temperatures.

The anomalous normal-state characterized by the striking power-law form of the resistivity close to p_c is unstable towards superconductivity at low temperatures (figure 4). Superconductivity in $CePd_2Si_2$ is inferred from the full loss of resistivity in two samples, with residual resistance ratios (RRR) of 34 and 55. Partial transitions were observed in two further samples with RRR 21 and 9.4, while no superconductivity was observed in samples with values of RRR less than 9. Figure 5(b) shows the transitions of these samples at $p \simeq p_c$. Increasing RRR gives rise to sharper transitions and higher values for T_c, indicating the importance of impurity scattering in breaking up the superconducting pairs. A study of the upper critical field as a function of temperature up to a field of 0.12 T on the sample with RRR = 34 leads to the conclusion that the initial slope $B'_{c2} \equiv dB_{c2}/dT$ must be much higher for $CePd_2Si_2$ than for conventional superconductors (figure 5(a)). The high slope, which is estimated to be of the order of 5 T K^{-1}, together with the low transition temperature, implies a short coherence length, which is consistent with a high effective mass of the quasiparticles forming Cooper pairs. A treatment analogous to that used in [38] gives $\xi^2 \simeq c(T_c B'_{c2})^{-1}$, where the constant $c \simeq 5 \times 10^4$ T Å^2. With $T_c \simeq 0.4$ K and $B'_{c2} \simeq 5$ T K^{-1}, we estimate the coherence length as $\xi \sim 150$ Å.

A detailed study of the phase boundaries $T_c(p)$ and $T_N(p)$ was carried out for one of these samples (RRR = 34) (figure 1). We find that T_c, taken at the 50% point of the resistive transition, goes through a single maximum at $p = 2.71$ GPa, just below the extrapolated critical pressure $p_c \simeq 2.86$ GPa. The curve $T_c(p)$ is approximately symmetric around its maximum and has a width of $\Delta p \simeq 0.8$ GPa. Measurements on the other fully and partially superconducting samples at selected pressures confirm this behaviour.

Full superconducting transitions can be observed even in the ordered state, where indications of both phase transitions are present in $\rho(T)$ (figure 4). However, the intriguing question, whether both transitions occur in the same region of the sample, or whether the two phases are mutually exclusive, cannot be answered straightforwardly from measurements of the resistivity alone.

3.2. $CeIn_3$

$CeIn_3$ shows a qualitatively similar behaviour to $CePd_2Si_2$, but a number of important differences are revealed on closer inspection. Again, we identify a high-temperature region, in which the resistivity is nearly constant and goes through a weak maximum near 70 K (figure 6). With decreasing temperature, the resistivity drops rapidly, and has a sharp anomaly at the Néel temperature of about 10 K. With increasing pressure, both temperatures shift, but while T_N
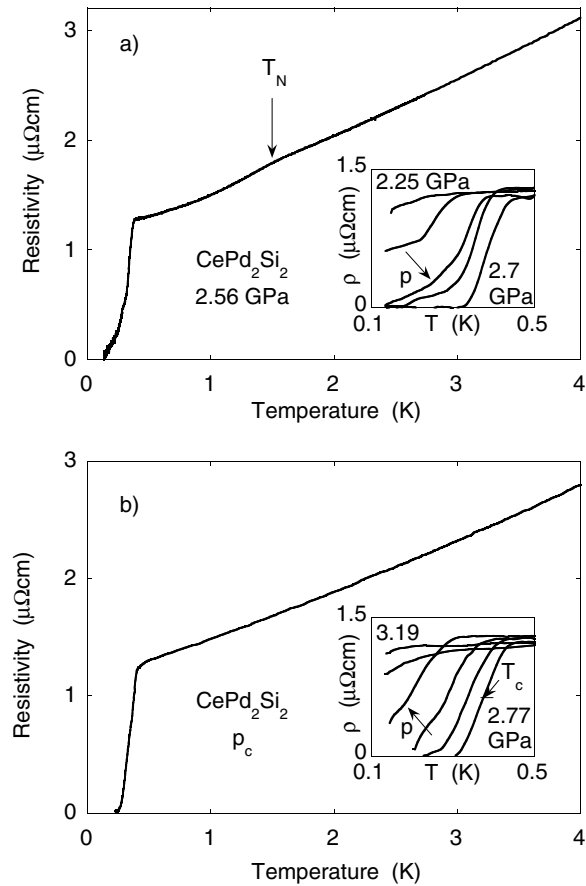
Figure 4. The low-temperature resistivity of $CePd_2Si_2$ measured along the *a*-axis (a) at 2.56 GPa, in the magnetic region of the phase diagram ($p < p_c$), where T_N is still visible as a kink in $\rho(T)$, and (b) at 2.8 GPa, very close to p_c. The insets show the development of the superconducting transition as the pressure is reduced (inset to (a)), and increased (inset to (b)) away from p_c.
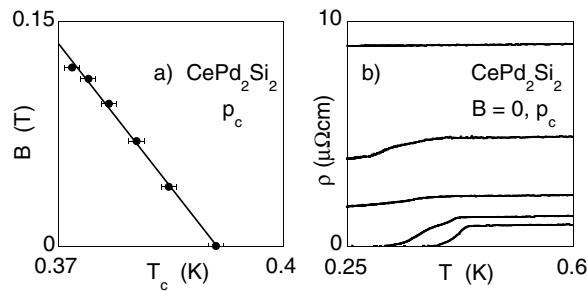

Figure 5. (a) The magnetic field dependence of T_c in $CePd_2Si_2$, determined at the 80% point of the resistive transition in small magnetic fields up to 0.12 T. The data indicate an initial slope of $B'_{c2} \simeq -5$ T K^{-1}. (b) The low-temperature resistivity in $CePd_2Si_2$ samples of varying purity, indicated by their low-temperature limiting normal-state resistivity, ρ_0. The two purest samples, with RRR $= 55$ and 34 show full superconducting transitions, while two more samples with RRR down to 10 show partial transitions. No trace of superconductivity is seen in samples with RRR < 9.
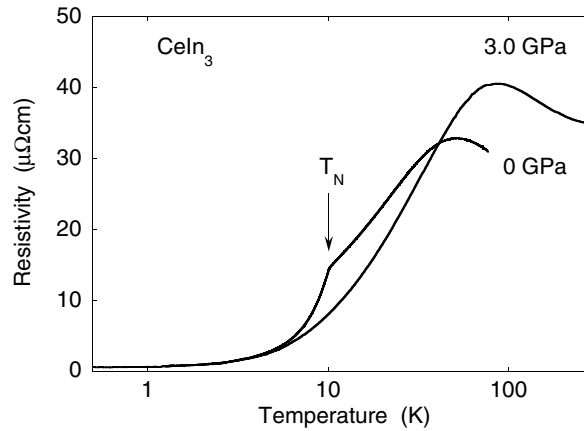
Figure 6. The resistivity of CeIn$_3$ at ambient pressure and at 3 GPa, just above the critical pressure $p_c \simeq 2.6$ GPa, plotted versus a logarithmic temperature scale. The magnetic transition temperature, T_N, marked by an arrow, is visible as a sudden change in slope and is extracted, as in the case of CePd$_2$Si$_2$, from the mid-point of dρ/dT. The maximum of $\rho(T)$ is only weakly T-dependent, compared to the case for CePd$_2$Si$_2$ and increases from about 70 K to about 100 K over the pressure range from 0 to 3 GPa.

is strongly pressure dependent and can be suppressed at a critical pressure $p_c \simeq 2.55$ GPa, the upper temperature scale T_{sf} appears to be much less pressure dependent, when compared to CePd$_2$Si$_2$. Over the pressure range from 0 to 3 GPa, the position of the maximum only changes from about 70 K to about 100 K.

In further contrast to CePd$_2$Si$_2$, the Néel temperature curve $T_N(p)$ (figure 2) is seen to be concave down at higher pressures, indicating a pressure dependence $T_N \propto (p_c - p)^x$ with exponent $x < 1$ and more in line with theoretical predictions for the role of 3D spin fluctuations in suppressing magnetic order. It was difficult to follow T_N below 3 K, because the transition was less clearly defined. It is likely that on approaching the critical pressure the increasing slope of $T_N(p)$ leads to a wider distribution of ordering temperatures within the sample due to inhomogeneities of sample composition and pressure. This in turn would give broader anomalies in the resistivity trace, making T_N more difficult to determine.

Close to the extrapolated critical pressure, sharp superconducting transitions are seen below 200 mK (figure 7). The superconducting region again reaches well into the ordered part of the phase diagram and is confined within about 0.5 GPa, with a maximum at 2.55 GPa.

The normal-state resistivity at low temperatures approaches the form predicted for a 3D antiferromagnet in the limit of very low temperatures ($T \ll T_{sf}$/RRR), $\Delta\rho \propto T^{3/2}$, only close to p_c and at low temperatures (figure 9—see later). The power-law exponent x returns to the Fermi-liquid value 2 more rapidly than in CePd$_2$Si$_2$, when the system is tuned away from the critical point, and does not lock into a constant value over a sizable temperature range.

4. Discussion

4.1. Normal-state resistivity

The normal-state data obtained in this study reveal interesting differences between the tetragonal system CePd$_2$Si$_2$ and the cubic CeIn$_3$. In CePd$_2$Si$_2$, the temperature dependence of the resistivity is characterized over nearly two orders of magnitude in temperature by a power
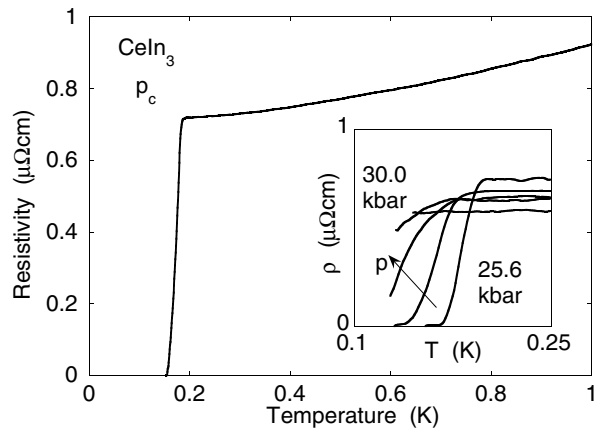
Figure 7. The low-temperature resistivity of CeIn$_3$ at $p_c \simeq 2.6$ GPa. The inset shows the development of the superconducting transition as the pressure is increased away from p_c.
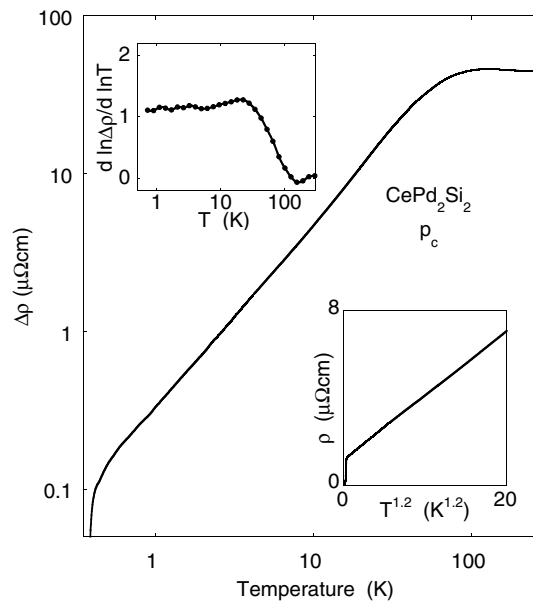

Figure 8. The resistivity of CePd$_2$Si$_2$ near p_c. The main figure shows $\Delta\rho \equiv \rho - \rho_0$ versus T on a doubly logarithmic scale, where the residual resistivity $\rho_0 \simeq 1.4$ $\mu\Omega$ cm was estimated by a fitting procedure applied to the normal-state, low-temperature data. The resistivity is essentially linear in $T^{1.2}$ over nearly two orders of magnitude in temperature down to the onset of a superconducting transition near 0.4 K (lower inset) and crosses over rapidly to a nearly constant value above about 40 K. The temperature-dependent exponent $x(T)$, extracted by taking the temperature logarithmic derivative of the resistivity, $x \equiv \partial \log(\rho - \rho_0)/\partial \log T$ (upper inset), exhibits a corresponding wide plateau close to 1.2 and a narrow crossover to 0 at high temperatures.

law $\rho = \rho_0 + AT^x$ with exponent x close to 1, and by a rapid crossover to a nearly constant resistivity at high temperatures (figure 8).

These properties of the tetragonal metal CePd$_2$Si$_2$ and its homologue CeNi$_2$Ge$_2$ contrast sharply with those of the cubic antiferromagnet CeIn$_3$ [20, 31]. In the latter, the resistivity

deviates from the Fermi-liquid form only in a very narrow pressure range near the critical pressure p_c. At p_c and in low magnetic fields the resistivity exponent, or more precisely $d \ln(\rho - \rho_0)/d \ln T$, grows smoothly with decreasing temperature and tends towards a value of about 3/2 near 1 K (figure 9). For the origin of this intriguing difference, we may consider first the known magnetic structure of CePd$_2$Si$_2$, which suggests a frustrated spin coupling along the c-axis and hence a strongly anisotropic spin-fluctuation spectrum [24, 25, 31] that may be more nearly 2D than 3D as expected for CeIn$_3$. For a comparison with the predictions of the standard magnetic interaction model, we consider first the limit in which regions about the 'hot spots' on the Fermi surface (those states whose self-energies can exhibit a non-Fermi-liquid form due to antiferromagnetic spin fluctuations) dominate the temperature dependence of the resistivity. This is expected to occur at very low temperatures $T \ll T_{sf}/\mathrm{RRR}$, when a short circuiting via normal regions of the Fermi surface is blocked for example by isotropic potential scattering via weak residual impurities. At a continuous antiferromagnetic critical point one then expects in the low-temperature limit $\Delta \rho \sim T^{d/z}$, where d is the effective dimension of the spin-fluctuation spectrum and z is the dynamical exponent normally taken to be 2 in our problem [6]. For this simplest model the resistivity exponent is thus expected to be 3/2 in 3D, in agreement with our observations on cubic CeIn$_3$, and unity for 2D, in closer agreement to the results on pure samples of the tetragonal CePd$_2$Si$_2$ and CeNi$_2$Ge$_2$. The precise degree of anisotropy can depend on details of the microscopic near-neighbour exchange constants, giving rise to the observed sample dependence of the power-law exponents.
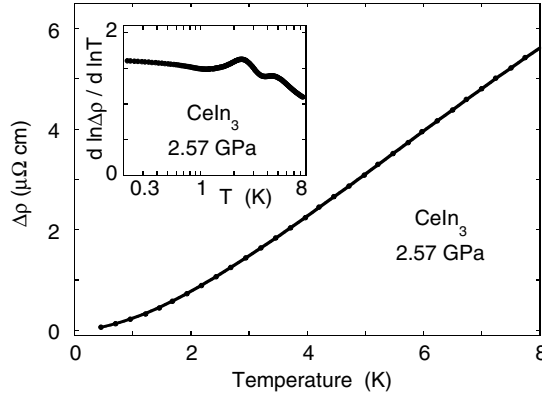

Figure 9. The resistivity of CeIn$_3$ near $p_c \simeq 2.6$ GPa. The main figure shows $\Delta \rho \equiv \rho - \rho_0$ versus T, where the residual resistivity $\rho_0 \simeq 0.6 \ \mu\Omega$ cm was estimated by a fitting procedure applied to the normal-state, low-temperature data. The inset shows the temperature-dependent exponent $x(T) \equiv \partial \log(\rho - \rho_0)/\partial \log T$, which exhibits a smooth crossover towards a low-temperature limiting value close to 3/2.

Further evidence for a quasi-two-dimensional character of the spin-fluctuation spectrum is drawn from the linear pressure dependence of T_N observed in CePd$_2$Si$_2$ close to p_c. In the magnetic interaction model [6] this would indicate an effective dimension close to 2, in agreement with the simplest interpretation of the resistivity data and with recent neutron scattering work on the related compound CeNi$_2$Ge$_2$ [39]. We note that by comparison $T_N(p)$ in CeIn$_3$ follows a power less than 1 close to p_c, consistent with $d = 3$ and with the observed low-temperature resistivity $\Delta \rho \sim T^{3/2}$. We stress that the dimensionality d refers to the magnetic fluctuation spectrum, not to the carriers, which remain unconstrained to move in 3D.

It may be instructive to relate the crystal and magnetic structures of our antiferromagnetic *metals* to those of the extensively studied *insulators* K$_2$NiF$_4$ and KNiF$_3$ [40]. Quasi-2D

magnetic behaviour has long been known to arise in the layered perovskite K_2NiF_4, in which the magnetic moments of Ni occupy bct positions and order with $Q = [\frac{1}{2}\frac{1}{2}0]$, in exact analogy to the position and ordering of the Ce moments in $CePd_2Si_2$. By contrast, its simple cubic counterpart $KNiF_3$ displays 3D magnetic behaviour and parallels $CeIn_3$ in the arrangement of the magnetic moments and in the ordering wavevector $Q = [\frac{1}{2}\frac{1}{2}\frac{1}{2}]$.

Because of competing contributions to the electrical conductivity from hot and cold regions on the Fermi surface, the intermediate-temperature regime is more complex. The standard treatment outlined above can be extended into this region [41, 42]. Here, one finds a temperature range in which exponents less than 3/2 can occur as a crossover between high- and low-temperature forms of $\rho(T)$ even for a 3D spin-fluctuation spectrum, but it is too early to tell whether or not it can account for all of the features that we observe, both in tetragonal $CePd_2Si_2$ and cubic $CeIn_3$, in a consistent way. In particular, we note that the power-law resistivity observed in $CePd_2Si_2$ at p_c extends to nearly 40 K, i.e. roughly 0.5 T_{sf}, and lies far outside the predictive range of the magnetic interaction model in its current form.

In a radical departure from the conventional model, an intuitive description of this strange metallic state could be based on a more extreme separation of the charge and spin degrees of freedom than is present in current approaches [43–45]. Convincing evidence is emerging that in at least one other Ce-based heavy-fermion system, the $CeCu_{6-x}Au_x$ series, the quantum critical point is accompanied by unexpected local spin dynamics [46, 47]. Within the standard magnetic interaction model the imaginary part of the wavevector- and frequency-dependent susceptibility is of the form $Im \chi(q, \omega) \sim g(q)\omega^\alpha$ at sufficiently low ω (>0) and T, where g is some function of q and $\alpha = 1$. In the standard model this value of α is expected to hold even in the limit $T_N \to 0$ provided that $d + z > 4$ [6]. However, for $CeCu_{6-x}Au_x$ it appears that in the low-temperature limit the exponent α is anomalous and significantly less than unity near the antiferromagnetic quantum critical point. Superficially, the slight deviation of α from its theoretical value (together with the observed ω/T scaling) might be seen as a minor correction, but on closer examination, a sublinear frequency dependence presents a major challenge to our present understanding of metallic magnetism and could imply a breakdown of Fermi-liquid theory of an entirely different order from that expected in any known model.

Inelastic neutron scattering on the pure, stoichiometric compound $CeNi_2Ge_2$ could decide whether such behaviour can occur in the absence of disorder and whether it is, ultimately, more widely spread in heavy-fermion systems on the threshold of magnetism.

4.2. Superconductivity and magnetism

The phase diagrams of $CePd_2Si_2$ and $CeIn_3$ show a striking dependence of superconductivity on magnetism (figures 1, 2). The superconducting 'bubble' appears to be tacked onto the threshold of magnetic order, suggesting that in these two systems, superconductivity is promoted, rather than hindered, by the magnetic interaction which is at its largest near p_c. The discovery of a wide high-pressure superconducting phase away from the critical point in the homologue to $CePd_2Si_2$, $CeNi_2Ge_2$ [26, 27], indicates, however, that the situation in $CePd_2Si_2$ may be complicated by a further superconducting state above p_c, beyond the range of our study. For simplicity, our discussion will focus on the narrow superconducting region near the critical pressure, the existence of which has been independently confirmed in both $CePd_2Si_2$ and $CeIn_3$ [32, 33, 48] and which appears most closely associated to the presence of strong magnetic fluctuations. Can we achieve at least a qualitative understanding of the salient results emerging from these studies: the confinement of superconductivity to a narrow region around p_c and to samples with purity levels exceeding a critical value?

We consider first the role of impurity scattering in destroying anisotropic superconductivity, as mean free paths shorter than the superconducting coherence length, ξ, rapidly suppress T_c. Because the sample quality enters as the fraction of coherence length over mean free path, longer coherence lengths limit superconductivity to purer samples. Closeness to the quantum critical point, in turn, determines the effective mass m^*, as evidenced by heat capacity measurements on related systems, and therefore ξ. The simplest mechanism explaining the demise of superconductivity away from p_c would therefore lie in the increase of ξ associated with the decrease in m^*. In the case of CePd$_2$Si$_2$, ξ is estimated at p_c to be around 150 Å, while the mean free path should go roughly as $\ell \simeq 1500$ Å $\mu\Omega$ cm/ρ_0 [38], becoming comparable to ξ for samples with a resistance ratio of the order of 10. These numbers are consistent with our finding that full transitions were confined to samples of CePd$_2$Si$_2$ with RRR larger than 10. Further, we can estimate the rate of decrease with pressure of $\xi \propto 1/m^* \propto 1/\gamma$, where γ is the Sommerfeld coefficient of the specific heat, C/T, from pressure measurements of γ on the related material CeNi$_2$Ge$_2$. In CeNi$_2$Ge$_2$, γ drops at an initial rate of about 0.2 J K^{-2} mol^{-1} GPa^{-1} from a zero-pressure value of about 0.4 J K^{-2} mol^{-1} [49]. Therefore, we can expect ξ approximately to double over a range of 1 GPa, which should be sufficient to destroy superconductivity in samples with RRR $\sim$ 20–30. These numbers are in order-of-magnitude agreement with the observed width of the superconducting region, but the fact that the cleanest sample, with RRR $\simeq$ 60, has a superconducting region no larger than the RRR $\simeq$ 30 sample suggests that further mechanisms may be limiting superconductivity in CePd$_2$Si$_2$.

One such influence may lie in the progressive competition from other coupling mechanisms, as the relative strength of the magnetic interaction decreases with distance from the critical point. Within the magnetic interaction model, superconductivity results from the dominance of the magnetic channel over all other channels of the quasiparticle interaction at the critical point. Moving away from p_c, however, T_c can diminish even in the absence of impurities, as competing channels, which may favour different pairing symmetries, become sufficiently strong to alter T_c dramatically.

While a similar mechanism may explain the confinement of superconductivity in CeIn$_3$ close to p_c and to pure samples, there is an interesting discrepancy between the maximum values of T_c in the two materials. Despite higher levels of purity and a similar value for T_{sf}, CeIn$_3$ has only half the T_c of CePd$_2$Si$_2$. The size of T_c depends critically on the coupling parameter λ_Δ, which involves the Cooper pair wavefunction and the strength of the quasiparticle interaction. In the case of phonon-mediated superconductivity, λ_Δ reduces to the mass enhancement $\lambda = (m^* - m)/m$, but it is a more complicated property in anisotropic superconductors. In accordance with recent numerical comparisons of the two- and three-dimensional case [50, 51], we speculate that CePd$_2$Si$_2$ has a more favourable optimum value for λ_Δ due to the more anisotropic and possibly nearly two-dimensional nature of its spin-fluctuation spectrum inferred from its normal-state properties.

One might naively expect that right at the critical pressure, nearly static modes around the ordering wavevector Q should be pair-breaking and reduce T_c to a local dip. Recent numerical calculations [50, 51], however, do not predict such a dip at least in the antiferromagnetic case, and indeed the data on both materials show no evidence of a minimum at p_c.

4.3. Implications for CeCu$_2$Si$_2$ and other rare-earth compounds

Magnetically mediated superconductivity may be expected to occur quite generally in nearly magnetic metals of sufficiently high purity. For many years, the scarcity of examples of superconductivity in 4f heavy-fermion systems that appeared to be on the border of magnetism

and that could be prepared in pure form seemed to contradict this expectation. After extensive investigations over nearly two decades superconductivity appeared to be limited solely to $CeCu_2Si_2$ and its twin $CeCu_2Ge_2$. The new findings on $CePd_2Si_2$, $CeRh_2Si_2$ [18] and $CeIn_3$ may help to shed light on the origin of this scarcity and to open the way to the discovery of many new examples.

The key point is that superconductivity may indeed be ubiquitous in heavy-fermion systems, as anticipated by the magnetic interaction model, but often only in very pure samples in a narrow range of lattice density or pressure on the very edge of magnetic order. A rapid collapse of superconductivity away from the critical density, or critical pressure p_c, may appear surprising but it is not incompatible with the magnetic interaction model for nearly antiferromagnetic metals. Within this model, T_c can fall with increasing $|p - p_c|$ because of

  (i) the decrease in the ratio of the mean free path to the superconducting coherence length as the quasiparticle mass renormalization factor falls,
 (ii) the decrease in the strength and the non-locality of magnetic interactions and thus the collapse of the pairing parameter λ_Δ and
(iii) the growing competition of other quasiparticle interaction channels.

Evidence for this precarious existence of superconductivity on the border of antiferromagnetism around *ambient* pressure has been seen in pure samples of $CeNi_2Ge_2$ [24, 29, 52]. In other nearly magnetic systems, however, the same phenomena may only be observed via tuning of the lattice density. This prescription has led to the discovery of superconductivity not only in the above systems, but more recently also in $CeCu_2$ [19], $CeCu_5Au$ [21], $CeRhIn_5$ and $CeIrIn_5$ [53].

The crucial parameter in this approach, the 'closeness' to the critical point, needs to be defined more accurately to check whether this scenario can apply even to the extreme case of *$CeCu_2Si_2$*. Amongst the many mechanisms under discussion, an intriguingly simple possibility is that $CeCu_2Si_2$ is nearly critical over a wide range in pressure, simply extending the phenomenon observed in $CeIn_3$ and $CePd_2Si_2$ up to about 10 GPa, in analogy to recent findings on $CeNi_2Ge_2$ and $CePd_2Si_2$ [24–29]. A detailed analysis of the evolution of the normal-state properties of $CeCu_2Si_2$ with high hydrostatic pressure is under way to see whether deviations from Fermi-liquid behaviour indeed extend over the entire superconducting range.

However, even if the correlation length decreases with distance from the quantum critical point, the mass enhancement associated with the magnetic interaction channel can still be large enough to allow magnetically mediated superconductivity, if competing channels are relatively weak and if the spin-fluctuation spectrum is soft over a wide range in momentum space. Low-lying modes over a large volume in q-space loosely imply a low dimensionality of the spin-fluctuation spectrum. They could arise from a nearly two-dimensional character of the spin-fluctuation spectrum, as is discussed for the case of $CePd_2Si_2$, or an isotropic but weak dispersion of the relaxation rate, Γ_q. This dispersion can be estimated from the spin-fluctuation temperature, which for $CeCu_2Si_2$ is much lower than in most of the other superconducting Ce compounds listed above.

In view of other low-dimensional superconducting correlated electron systems, the former route is of particular interest. Quantitative, numerical comparisons of the superconducting transition temperature for two- and three-dimensional nearly antiferromagnetic metals indicate a significant enhancement of T_c for lower dimensionality [50, 51]. As a guiding principle, this approach leads naturally to searching for magnetically mediated superconductivity in 2D materials and would seem consistent with the recent discovery of superconductivity at surprisingly high T_c in two new heavy-fermion compounds, $CeIrIn_5$ and $CeRhIn_5$, which form in a layered structure and appear to be two-dimensional relatives of the cubic system $CeIn_3$ [53].

5. Conclusions

$CePd_2Si_2$ and $CeIn_3$ present a unique opportunity to investigate the implications of lattice structure and magnetic anisotropy for the superconducting and normal-state properties on the threshold of magnetism.

At p_c, both materials exhibit an anomalous normal state extending from an upper temperature scale T_{sf} of the order of 100 K down to the onset of superconductivity below 430 mK and 175 mK, respectively. The behaviour of the resistivity of $CePd_2Si_2$ is particularly striking: it exhibits a nearly linear temperature dependence over about two orders of magnitude in temperature.

The superconducting state is characterized by its closeness to the border of antiferromagnetic order. This link is underlined by the small size of the superconducting region in both materials, indicating a likely magnetic origin for the attractive interaction responsible for the formation of Cooper pairs. The wide separation between T_{sf} and T_c could make these systems amenable to a theoretical treatment of the superconducting transition.

Superconductivity in rare-earth-based heavy-fermion metals is still a rare phenomenon. The general phase diagram observed in $CePd_2Si_2$ and $CeIn_3$ may provide the quantitative understanding necessary to unravel other strongly correlated electron systems, including $CeCu_2Si_2$.

Acknowledgments

References

[1] Steglich F, Aarts J, Bredl C D, Lieke W, Meschede D, Franz W and Schäfer J 1979 *Phys. Rev. Lett.* **43** 1892
[2] Trovarelli O, Weiden M, Müller-Reisener R, Gómez-Berisso M, Gegenwart P, Deppe M, Geibel C, Sereni J G and Steglich F 1997 *Phys. Rev.* B **56** 678
[3] Knebel G, Eggert C, Engelmann D, Viana R, Krimmel A, Dressel M and Loidl A 1996 *Phys. Rev.* B **53** 11 586
[4] Gegenwart P, Langhammer C, Geibel C, Helfrich R, Lang M, Sparn G, Steglich F, Horn R, Donnevert L, Link A and Assmus W 1998 *Phys. Rev. Lett.* **81** 1501
[5] Jaccard D, Behnia K and Sierro J 1992 *Phys. Lett.* A **163** 475
[6] Lonzarich G G 1997 *Electron* ed M Springford (Cambridge: Cambridge University Press)
[7] Moriya T 1985 *Spin Fluctuations in Itinerant Electron Magnetism* (New York: Springer)
[8] Hertz J 1976 *Phys. Rev.* B **14** 1164
[9] Pfleiderer C, McMullan G J, Julian S R and Lonzarich G G 1997 *Phys. Rev.* B **55** 8330
[10] Ishikawa Y, Noda Y, Uemura Y J, Majkrzac C F and Shirane G 1985 *Phys. Rev.* B **31** 5884
[11] Lonzarich G G and Taillefer L 1985 *J. Phys. C: Solid State Phys.* **18** 4339
[12] Lonzarich G G 1986 *J. Magn. Magn. Mater.* **54–57** 612
[13] Grosche F M, Pfleiderer C, Lonzarich G G and Bernhoeft N R 1995 *Physica* B **206+207** 22
[14] Bernhoeft N R, Lonzarich G G, Mitchell P W and Paul D M^{c}K 1983 *Phys. Rev.* B **28** 422
[15] Bernhoeft N R, Law S A, Lonzarich G G and Paul D M^{c}K 1988 *Phys. Scr.* **38** 191
[16] Lonzarich G G, Bernhoeft N R, Hayden S M and Paul D M^{c}K 1989 *Physica* B **156+157** 699
[17] Grosche F M, Julian S R, Mathur N D and Lonzarich G G 1996 *Physica* B **223+224** 50
[18] Movshovich R, Graf T, Mandrus D, Thompson J D, Smith J L and Fisk Z 1996 *Phys. Rev.* B **53** 8241
[19] Vargoz E, Link P, Jaccard D, LeBihan T and Heathman S 1997 *Physica* B **229** 225
[20] Walker I R, Grosche F M, Freye D M and Lonzarich G G 1997 *Physica* C **282–287** 303
[21] Wilhelm H, Raymond S, Jaccard D, Stockert O and von Löhneysen H 1999 *Preprint* cond-mat/9908442

[22] Morin P, Vettier C, Flouquet J, Konczykowski M, Lassailly Y, Mignot J-M and Welp U 1988 *J. Low Temp. Phys.* **70** 377

[23] Knebel G, Brando M, Hemberger J, Nicklas M, Trinkl W and Loidl A 1999 *Phys. Rev.* B **59** 12 390

[24] Grosche F M, Agarwal P, Julian S R, Wilson N J, Haselwimmer R K W, Lister S J S, Mathur N D, Carter F V, Saxena S S and Lonzarich G G 1998 *Preprint* cond-mat/9812133

[25] Grosche F M, Agarwal P, Julian S R, Wilson N J, Haselwimmer R K W, Lister S J S, Mathur N D, Carter F V, Saxena S S and Lonzarich G G 2000 *J. Phys.: Condens. Matter* **12** L533

[26] Grosche F M, Lister S J S, Carter F V, Haselwimmer R K W, Saxena S S, Mathur N D, Julian S R and Lonzarich G G 1997 *Physica* B **239** 62

[27] Lister S J S, Grosche F M, Carter F V, Haselwimmer R K W, Saxena S S, Mathur N D, Julian S R and Lonzarich G G 1997 *Z. Phys.* B **103** 263

[28] Agarwal P, Grosche F M, Haselwimmer R K W, Lister S J S, Carter F V, Saxena S S, Julian S R and Lonzarich G G 2001 to be published

[29] Braithwaite D, Fukuhara T, Demuer A, Sheikin I, Kambe S, Brison J-P, Maezawa K, Naka T and Flouquet J 2000 *J. Phys.: Condens. Matter* **12** 1339

[30] Raymond S, Jaccard D, Wilhelm H and Cerny R 1999 *Solid State Commun.* **112** 617

[31] Mathur N D, Grosche F M, Julian S R, Walker I R, Freye D M, Haselwimmer R K W and Lonzarich G G 1998 *Nature* **394** 39

[32] Sheikin I, Steep E, Braithwaite D, Brison J-P, Raymond S, Jaccard D and Flouquet J 2001 *J. Low Temp. Phys.* at press

[33] Demuer A *et al* 2001 to be published

[34] Grier B H, Lawrence J M, Murgai V and Parks R D 1984 *Phys. Rev.* B **29** 2664

[35] Thompson J D, Parks R D and Borges H 1986 *J. Magn. Magn. Mater.* **54–57** 377

[36] Smith T F, Chu C W and Maple M B 1969 *Cryogenics* **9** 53

[37] Mathur N D 1995 *PhD Thesis* University of Cambridge

[38] Rauchschwalbe U 1986 *PhD Thesis* Technical University of Darmstadt

[39] Fåk B, Flouquet J, Lapertot G, Fukuhara T and Kadowaki H 2000 *J. Phys.: Condens. Matter* **12** 5423

[40] Lines M E 1967 *Phys. Rev.* B **164** 736

[41] Hlubina R and Rice T M 1995 *Phys. Rev.* B **51** 9253

[42] Rosch A 1999 *Phys. Rev. Lett.* **82** 4280

[43] Coleman P 1999 *Physica* B **261** 353

[44] Anderson P W 1997 *Theory of Superconductivity of High-T_c Cuprate Superconductors* (Princeton, NJ: Princeton University Press)

[45] Si Q, Smith J and Ingersent K 1999 *Int. J. Mod. Phys.* B **13** 2331

[46] Schröder A, Aeppli G, Bucher E, Ramazashvili R and Coleman P 1998 *Phys. Rev. Lett.* **80** 5623

[47] Schröder A, Aeppli G, Coldea R, Stocker O, von Löhneysen H, Bucher E, Ramazashvili R and Coleman P 2000 *Nature* **407** 351

[48] Knebel G, Braithwaite D, Canfield P, Lapertot G and Flouquet J 2001 *Phys. Rev.* B submitted

[49] Hellmann P, Donnevert L, Thomas S, Geibel C, Sparn G and Steglich F 1996 *Czech. J. Phys.* **46** 2591

[50] Monthoux P and Lonzarich G G 1999 *Phys. Rev.* B **59** 14 598

[51] Monthoux P and Lonzarich G G 2001 *Phys. Rev.* B **63** 054 529

[52] Gegenwart P, Kromer F, Lang M, Sparn G, Geibel C and Steglich F 1999 *Phys. Rev. Lett.* **82** 1293

[53] Hegger H, Petrovic C, Moshopoulou E G, Hundley M F, Sarrao J L, Fisk Z and Thompson J D 2000 *Phys. Rev. Lett.* **84** 4986